IEICE TRANS. FUNDAMENTALS, VOL.E91–A, NO.4 APRIL 2008

PAPER

Boundary Conditions for Numerical Stability Analysis of Periodic Solutions of Ordinary Differential Equations

Sunao MURASHIGE[†a)], ***Member***

SUMMARY This paper considers numerical methods for stability analyses of periodic solutions of ordinary differential equations. Stability of a periodic solution can be determined by the corresponding monodromy matrix and its eigenvalues. Some commonly used numerical methods can produce inaccurate results of them in some cases, for example, near bifurcation points or when one of the eigenvalues is very large or very small. This work proposes a numerical method using a periodic boundary condition for vector fields, which preserves a critical property of the monodromy matrix. Numerical examples demonstrate effectiveness and a drawback of this method.

key words: *periodic solution, ordinary differential equations, stability, boundary conditions, numerical computation*

1. Introduction

Numerical stability analyses of periodic solutions often help us systematically understand complicated nonlinear phenomena including chaos (for example, [5]). This work focuses on stability of periodic solutions of ordinary differential equations

$$\frac{\mathrm{d}x}{\mathrm{d}t} = f(x) \quad \text{with } x(t=0) = x_0, \tag{1}$$

where $x \in \mathbb{R}^n$ and $f : \mathbb{R}^n \to \mathbb{R}^n$ is of class C^2. A solution of Eq. (1) can be expressed as $x(t) = \varphi_t(x_0) = \varphi(t, x_0)$, and a periodic solution $x(t)$ with period T satisfies $x(t) = x(t+T)$. First variations of this periodic solution follow the variational equations

$$\frac{\mathrm{d}X}{\mathrm{d}t} = \left.\frac{\partial f}{\partial x}\right|_{x=\varphi_t(x_0)} X \quad \text{with } X(t=0) = I, \tag{2}$$

where $X \in \mathbb{R}^{n\times n}$ and $I \in \mathbb{R}^{n\times n}$ denotes the identity matrix. In particular, stability of a periodic solution $x(t) = \varphi_t(x_0)$ with the period T is determined by the monodromy matrix $X(T)$, which is the solution of Eq. (2) at $t = T$, and its eigenvalues, Floquet multipliers. Thus, we can examine stability of periodic solutions using Eqs. (1) and (2).

In the standard numerical stability analyses of periodic solutions of Eq. (1), both Eqs. (1) and (2) are simultaneously solved with a suitable boundary condition, for example $\varphi_T(x_0) = x_0$. Seydel [8], Fairgrieve and Jepson [2], and Lust [6] pointed out that some commonly used numerical methods can give incorrect eigenvalues of the monodromy matrix $X(T)$ near bifurcation points, or when one of the eigenvalues is very large or very small. They considered this problem on the assumption that computed periodic solutions of Eq. (1) are accurate enough, and showed some reliable numerical methods using some ideas of numerical linear algebra. On the other hand, it should be noted that, even if periodic solutions of Eq. (1) are approximated with enough accuracy, this problem can occur and some critical properties of the monodromy matrix $X(T)$ cannot be preserved as shown in Sect. 5.1. This suggests that we may not be able to significantly improve accuracy of the approximate monodromy matrix $\tilde{X}(\tilde{T})$ only with highly accurate numerical schemes for differential Eqs. (1) and (2). Then this work tries to change the boundary condition so that some conditions of the monodromy matrix $X(T)$ are directly taken into consideration.

In this paper, Sect. 2 summarizes some relations among $\varphi_t(x_0)$, $X(t)$, and f, and some critical properties of the monodromy matrix $X(T)$. Section 3 shows a numerical method to obtain periodic solutions and $X(T)$ using a periodic boundary condition for the vector field f, which preserves a critical property of $X(T)$. Section 4 demonstrates computed results using the proposed method for the Van der Pol - Duffing equations. Section 5 discusses boundary conditions for Eqs. (1) and (2) in detail.

2. The Variational Equations and the Monodromy Matrix

This section summarizes critical properties of the matrix $X(t)$, which is a solution of Eq. (2). First, $X(t)$ can be related to the corresponding solution $x(t) = \varphi_t(x_0)$ of Eq. (1) as follows [7]:

Theorem 1: Let $X_{x_0}(t)$ denote the solution of Eq. (2) for a solution $x(t) = \varphi_t(x_0)$ of Eq. (1) with $x(t=0) = x_0$.

(a) The solution $X_{x_0}(t)$ of Eq. (2) can be expressed as

$$X_{x_0}(t) = \frac{\partial \varphi_t}{\partial x_0}. \tag{3}$$

(b) The solution $\varphi_t(x_0)$ of Eq. (1) can be related to $X_{x_0}(t)$ using the vector field f of Eq. (1) by

$$f(\varphi_t(x_0)) = X_{x_0}(t) f(x_0). \tag{4}$$

□

Manuscript received October 18, 2007.

[†]The author is with the Department of Complex Systems, School of Systems Information Science, Future University-Hakodate, Hakodate-shi, 041-8655 Japan.

a) E-mail: murasige@fun.ac.jp

DOI: 10.1093/ietfec/e91–a.4.1162

Stability of a periodic solution $x(t) = \varphi_t(x_0)$ with the period T of Eq. (1) is determined by the corresponding monodromy matrix $X_{x_0}(T)$ and its eigenvalues, which have the following properties [7]:

Theorem 2:

(a) One of eigenvalues of the monodromy matrix $X_{x_0}(T)$ is unity, and the associated eigenvector is $f(x_0)$, namely the tangent vector of the solution curve at x_0.

(b) For two different points $x_0, y_0 \in \mathbb{R}^n$ on an orbit of periodic solutions, there exists a non-singular matrix R such that $RX_{x_0}(T) = X_{y_0}(T)R$, namely $X_{x_0}(T)$ being similar to $X_{y_0}(T)$. Thus the eigenvalues of $X_{x_0}(T)$ are the same as those of $X_{y_0}(T)$.

□

A periodic solution is unstable if the largest absolute value of eigenvalues of $X(T)$ is greater than unity. Thus it is crucial to catch Theorem 2(a) in numerical stability analysis. Theorem 2(a) can be proved using Eq. (4). Also, since choice of x_0 on a periodic orbit is not unique, it is important to take Theorem 2(b) into consideration as shown in Sect. 4.

Next section derives a periodic boundary condition for the vector field f, which is directly related to Theorem 2(a), and proposes a computational method to obtain solutions of Eqs. (1) and (2) using it.

3. Periodic Boundary Conditions and Computational Methods

There are some computational methods, for example, the multiple shooting method or the collocation method, to obtain solutions of Eqs. (1) and (2) [5]. These methods use the same periodic boundary condition. The aim of this work is to modify the periodic boundary condition such that some critical properties of the monodromy matrix are preserved in computed results. For that, this work follows the simplest computational method, namely the simple shooting method, to avoid unnecessary complexity.

3.1 The Simple Shooting Method

Let a cross section Σ ($\ni x_0$) be transversal to an orbit of periodic solutions in the state space and given by

$$\Sigma = \{x \in \mathbb{R}^n \ : \ g(x) = 0\}. \tag{5}$$

A periodic solution can be determined by x_0 and T, namely the point x_0 on the orbit and the period T, which are solutions of

$$\begin{cases} \text{(a) periodic condition} & : & \varphi(T, x_0) - x_0 & = & 0, \\ \text{(b) phase condition} & : & g(x_0) & = & 0. \end{cases} \tag{6}$$

Approximate solutions $\tilde{x}_0$ and $\tilde{T}$ of the above equations can be obtained using Newton's method with suitable initial conditions. Here $\varphi(T, x_0)$ is a solution of the initial value problem Eq. (1) and can be numerically solved, for example, using the Runge-Kutta method. Then the variational Eqs. (2) are simultaneously solved with Eq. (1) using the same numerical method as that for Eq. (1) to obtain the monodromy matrix $X(T)$. This is the simple shooting method.

3.2 The Proposed Method

Computed results by the simple shooting method, namely approximate solutions $\tilde{x}_0$ and $\tilde{T}$ of Eq. (6) do not always produce the approximate monodromy matrix $\tilde{X}_{\tilde{x}_0}(\tilde{T})$ which satisfies Theorem 2 with enough accuracy, as shown in Sect. 4. This work tries to improve accuracy of $\tilde{X}_{\tilde{x}_0}(\tilde{T})$ using transformation of the periodic boundary condition (6.a) with Eq. (4).

If x_0 and T satisfy the periodic boundary condition (6.a), then the following equality stands:

$$f(\varphi(T, x_0)) - f(x_0) = 0. \tag{7}$$

Here it should be noted that, although approximate solutions $\bar{x}_0$ and $\bar{T}$ of Eq. (7) and the phase condition (6.b) do not necessarily satisfy (6.a), there exists a neighbourhood of exact solutions ${x_0}^*$ and T^* in which $\bar{x}_0$ and $\bar{T}$ satisfy (6.a). Using Eq. (4), the first term $f(\varphi(T, x_0))$ of the left hand side of Eq. (7) can be rewritten in the form

$$X_{x_0}(T)f(x_0) - f(x_0) = 0. \tag{8}$$

This corresponds to Theorem 2(a) and can be considered as the periodic boundary condition for the vector field f. The idea to improve the accuracy of $\tilde{X}_{\tilde{x}_0}(\tilde{T})$ is to adopt (8) as the periodic boundary condition. That is, instead of (6), we use the following boundary conditions:

$$\begin{cases} \text{(a) periodic condition} \ : \\ \qquad\qquad X_{x_0}(T)f(x_0) - f(x_0) = 0, \\ \text{(b) phase condition} \ : \qquad\quad g(x_0) = 0. \end{cases} \tag{9}$$

It should be noted that the periodic boundary condition (9.a) includes a solution $X_{x_0}(T)$ of the variational Eq. (2), which is not in (6.a). We may expect that Newton's method for (9) with good initial values of x_0 and T gives accurate approximate solutions $\tilde{x}_0$ and $\tilde{T}$, for which $\tilde{X}_{\tilde{x}_0}(\tilde{T})$ satisfies Theorem 2(a). Also it should be noted that both Eqs. (1) and (2) are simultaneously solved to obtain $X_{x_0}(T)$ in (9.a).

4. Numerical Examples

This section shows some computed results for the Van der Pol - Duffing equations

$$\begin{aligned} \frac{\mathrm{d}x}{\mathrm{d}t} &= f_1(x, y) = y, \\ \frac{\mathrm{d}y}{\mathrm{d}t} &= f_2(x, y) = -\{(x^2 - k)y \\ &\qquad + c_1 x + c_2 x^2 + x^3 + b_0\}. \end{aligned} \tag{10}$$

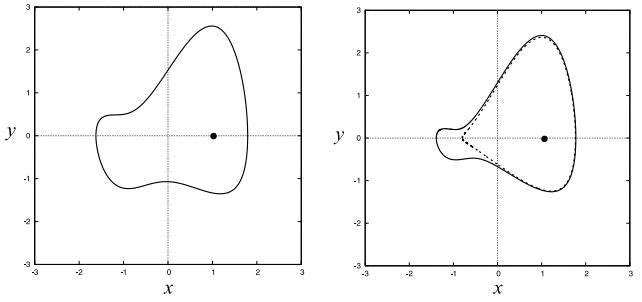

(a) $c_1 = -1.0$ (b) $c_1 = -1.12$

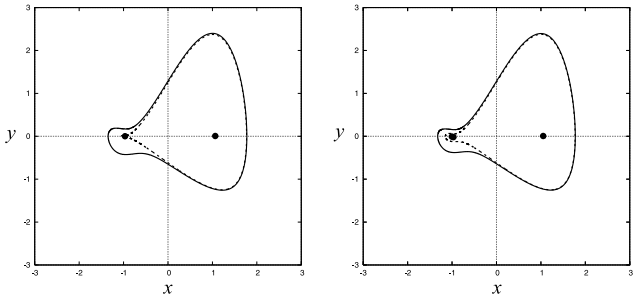

(c) $c_1 = -1.128$ (d) $c_1 = -1.129$

Fig. 1 Orbits of computed periodic solutions of Eq. (10) in the state space. $k = 0.897258546$, $c_2 = 0.87$, $b_0 = -1.0$, $x_0 \in \Sigma_-$. Σ_-: The negative x-axis. Solid line: stable, broken line: unstable, black circle: equilibrium points x_e. The convergence condition of Newton's method is $\|F(\tilde{u}, \tilde{\tau})\| < 10^{-7}$. The time increment of the Runge-Kutta method is $\Delta t = 0.005$.

This is a mathematical model for nonlinear oscillations. Stability of periodic solutions of Eq. (10) has been well investigated [1], [3]. This work focuses on numerical computation of periodic solutions near a homoclinic orbit of Eq. (10) which approaches an equilibrium point x_e as $t \to \pm\infty$.

4.1 Computed Results Using the Simple Shooting Method

Set the cross-section Σ along the x-axis, namely

$$\Sigma = \{(x, y) \in \mathbb{R}^2 \ : \ g(x, y) = y = 0\}, \tag{11}$$

and express the associated $x_0 \in \Sigma$ and $\varphi_t(x_0)$ as

$$x_0 = (u, 0), \quad \varphi_t(x_0) = (\varphi_1(t, u), \varphi_2(t, u)). \tag{12}$$

Then the conditions (6) of the simple shooting method can be written in the form

$$\begin{aligned} F_1(u, \tau) &= \varphi_1(\tau, u) - u = 0, \\ F_2(u, \tau) &= \varphi_2(\tau, u) \quad\ = 0. \end{aligned} \tag{13}$$

Solutions u^* and τ^* of $F(u, \tau) = (F_1(u, \tau), F_2(u, \tau)) = 0$ give a point $x_0 = (u, 0)$ on an orbit of a periodic solution and its period $T = \tau^*$. Approximate solutions $\tilde{u}$ and $\tilde{\tau}$ of $F(u, \tau) = 0$ can be obtained using Newton's method with suitable initial values (see Appendix).

Figure 1 shows some computed orbits of periodic solutions in the state space. In these computations, only c_1 is varied and the other parameters k, c_2 and b_0 are fixed to $k = 0.897258546$, $c_2 = 0.87$, $b_0 = -1.0$, respectively. These orbits are computed using the simple shooting method in which $x_0 = (u, 0)$ is located on the negative x-axis Σ_-, namely $u < 0$. The convergence condition of Newton's method for (13) is set to $\|F(\tilde{u}, \tilde{\tau})\| < 10^{-7}$ where $\|\ \|$ denotes the maximum norm. The initial value problems (1) and (2) are solved using the 4th order Runge-Kutta method with the time increment $\Delta t = 0.005$. Figure 1 shows that stable and unstable periodic orbits coexist in some parameter region, and that periodic orbits near a homoclinic orbit exist near $c_1 = -1.128$. Figures 2(a) and (b) show time series of computed periodic solutions away from and near a homoclinic orbit, respectively. Periodic solutions near a homoclinic orbit can be characterized by coexistence of slow motion near an equilibrium point x_e and fast motion away from x_e. Figures 3(a) and (b) show one parameter bifurcation diagrams for different values of k in (c_1, x_0) and (c_1, T), respectively. This work considers variation of stability of periodic solutions for $k = k_1 = 0.897258546$ with change of c_1. It should be noted that the period T of these solutions are very long near a homoclinic orbit.

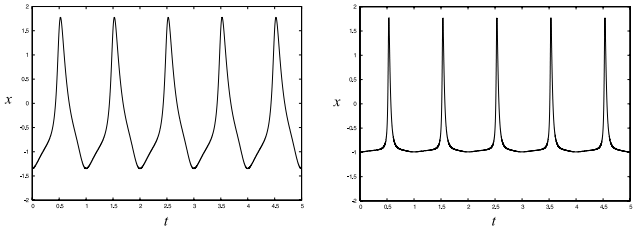

(a) $c_1 = -1.128$, stable (b) $c_1 = -1.1279$, unstable

Fig. 2 Time series of computed periodic solutions of Eq. (10). (a) and (b) correspond to periodic solutions away from and near a homoclinic orbit, respectively. The time t is normalized by the period T. See parameter values in Fig. 1.

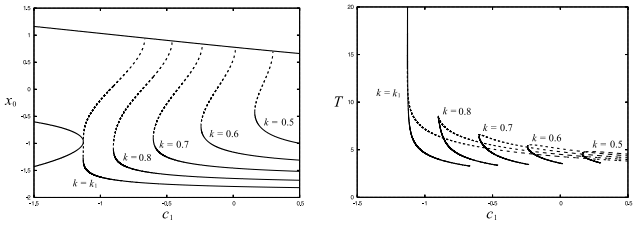

(a) (c_1, x_0) (b) (c_1, T)

Fig. 3 One parameter bifurcation diagrams. $k_1 = 0.897258546$. Solid line: stable, broken line: unstable, thick line in (a): equilibrium points. See parameter values in Fig. 1.

Figure 4 shows variation of computed eigenvalues μ_1 and μ_2 of the monodromy matrices $X(T)$ of unstable periodic orbits with change of c_1. Values of fixed parameters k, c_2 and b_0 are the same as those in Fig. 1. Figures 4(a) and (b) show the computed results for (a) $x_0 = (u, 0)$ with $u < 0$ on the negative x-axis Σ_- and (b) $x_0 = (u, 0)$ with $u > 0$ on the positive x-axis Σ_+, respectively. The left end of (a.1) and (b.1), at which $\mu_1 = \mu_2 = 1$, corresponds to the saddle node

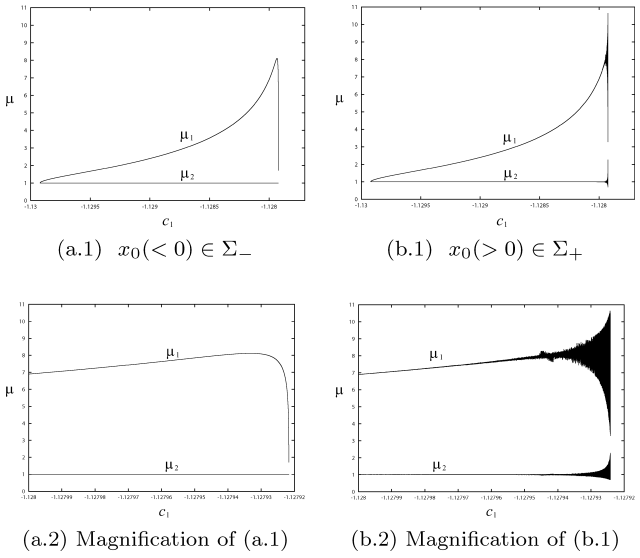

(a.1) $x_0(<0) \in \Sigma_-$ (b.1) $x_0(>0) \in \Sigma_+$

(a.2) Magnification of (a.1) (b.2) Magnification of (b.1)

Fig. 4 Variation of computed eigenvalues μ_1 and μ_2 of the monodromy matrix $X(T)$ for unstable periodic orbits with c_1. $X(T)$ is computed using the simple shooting method. See parameter values in Fig. 1.

bifurcation point. It is found that eigenvalues μ_1 and μ_2 for $x_0 \in \Sigma_-$ differ from those for $x_0 \in \Sigma_+$, and that computed results in Fig. 4(b) wiggle near $c_1 = -1.128$, namely near homoclinic orbits. That is, Theorems 2(a) and (b) are not satisfied in these results.

For $x_0 = (u, 0) \in \Sigma_\pm$, the right hand side of Eq. (10) has the form $f(x_0) = f(u, 0) = (f_1(u, 0), f_2(u, 0)) = (0, f_2(u, 0))$. Hence, from Theorem 2(a), $(0, 1)$ is the eigenvector of the exact monodromy matrix $X^*(T)$ for the trivial eigenvalue, namely unity, for the cross-sections $\Sigma_\pm$. Then $X^*(T)$ can be written in the form

$$X^*(T) = \begin{pmatrix} \lambda & 0 \\ \nu & 1 \end{pmatrix} \qquad (\lambda, \nu \in \mathbb{R}), \tag{14}$$

and its exact eigenvalues are $\mu_1^* = \lambda$ and $\mu_2^* = 1$. On the other hand, the computed monodromy matrices $\tilde{X}_{\Sigma_-}(\tilde{T})$ for $x_0 \in \Sigma_-$ and $\tilde{X}_{\Sigma_+}(\tilde{T})$ for $x_0 \in \Sigma_+$ at $c_1 \simeq -1.1279$ in Fig. 4 and the corresponding eigenvalues $\tilde{\mu}_{1,2}$ were

$$\begin{aligned} \tilde{X}_{\Sigma_-}(\tilde{T}) &= \begin{pmatrix} 7.452391 \times 10^0 & 3.063650 \times 10^{-5} \\ -4.249727 \times 10^0 & 1.000006 \times 10^0 \end{pmatrix} \\ &\to \begin{pmatrix} \tilde{\mu}_1 \\ \tilde{\mu}_2 \end{pmatrix} = \begin{pmatrix} 7.452371 \\ 1.000026 \end{pmatrix} \\ \tilde{X}_{\Sigma_+}(\tilde{T}) &= \begin{pmatrix} 4.739392 \times 10^0 & 1.857297 \times 10^{-8} \\ -1.562104 \times 10^8 & 9.603016 \times 10^{-1} \end{pmatrix} \\ &\to \begin{pmatrix} \tilde{\mu}_1 \\ \tilde{\mu}_2 \end{pmatrix} = \begin{pmatrix} 3.667826 \\ 2.031868 \end{pmatrix} \end{aligned} \tag{15}$$

These results show that the (2,1) element $\tilde{\nu}$ of $\tilde{X}(\tilde{T})$ can take a large value of the order of 10^8, and that the (2,2) element of $\tilde{X}(\tilde{T})$ can deviate from unity. Next section considers effects of the coordinate transformation on these results.

4.2 Transformation of the Van der Pol-Duffing Equations

This section considers a simple coordinate transformation given by

$$\boldsymbol{x} = Q\hat{\boldsymbol{x}} \quad \text{with } Q = \begin{pmatrix} 1 & 0 \\ 0 & \rho \end{pmatrix}, \tag{16}$$

where $\boldsymbol{x} = (x, y)^\top$, $\hat{\boldsymbol{x}} = (\hat{x}, \hat{y})^\top$ and $\rho \in \mathbb{R}\backslash\{0\}$, respectively. This corresponds to scaling in the y-direction. When the Van der Pol - Duffing Eq. (10) is expressed as $\mathrm{d}\boldsymbol{x}/\mathrm{d}t = \boldsymbol{f}(\boldsymbol{x}) = (f_1(x, y), f_2(x, y))^\top$, the transformed equations can be written in the form

$$\frac{\mathrm{d}\hat{\boldsymbol{x}}}{\mathrm{d}t} = \hat{\boldsymbol{f}}(\hat{\boldsymbol{x}}) = \begin{pmatrix} \hat{f}_1(\hat{x}, \hat{y}) \\ \hat{f}_2(\hat{x}, \hat{y}) \end{pmatrix} = Q^{-1}\, \boldsymbol{f}(Q\hat{\boldsymbol{x}}). \tag{17}$$

The monodromy matrices $X(T)$ for the original Eq. (10) and $\hat{X}(T)$ for the transformed Eq. (17) are related by

$$\hat{X}(T) = Q^{-1}X(T)Q = \begin{pmatrix} \lambda & 0 \\ \frac{1}{\rho}\nu & 1 \end{pmatrix}. \tag{18}$$

Thus the eigenvalues of $X(T)$ are the same as those of $\hat{X}(T)$, and the absolute value of the (2,1) element $|\nu/\rho|$ of $\hat{X}(T)$ can be reduced for $|\rho| > 1$. We may expect that this coordinate transformation (16) helps us decrease errors found in Fig. 4(b) and (15). Next section compares computed results for Eq. (17) with $\hat{x}_0 \in \Sigma_+$ using the simple shooting method and the proposed method in Sect. 3.2.

4.3 Computed Results Using the Proposed Method

The periodic boundary conditions for Eq. (17) in the proposed method in Sect. 3.2 can be obtained as follows. When $\hat{x}_0 \in \Sigma$ is located on the $\hat{x}$-axis, namely $\hat{y} = \hat{f}_1(\hat{x}_0) = 0$, Eq. (7) can be written in the form

$$\begin{aligned} \hat{f}_1(\hat{\varphi}_\tau(\hat{x}_0)) &= 0, \\ \hat{f}_2(\hat{\varphi}_\tau(\hat{x}_0)) - \hat{f}_2(\hat{x}_0) &= 0. \end{aligned} \tag{19}$$

Using Eq. (4), we can get

$$\begin{aligned} H_1(u, \tau) &= \sum_{j=1}^{2} \hat{X}_{1j}(\tau)\hat{f}_j(u) = 0, \\ H_2(u, \tau) &= \sum_{j=1}^{2} \hat{X}_{2j}(\tau)\hat{f}_j(u) - \hat{f}_2(u) = 0. \end{aligned} \tag{20}$$

where $(\hat{X}_{ij}(t)) = \hat{X}(t) = \partial\hat{\varphi}_t/\partial\hat{x}_0$ and $\hat{f}(u) = \hat{f}(\hat{x}_0 = (u, 0))$, respectively. We can obtain approximate solutions $\tilde{u}$ and $\tilde{\tau}$ of $H(u, \tau) = 0$ using Newton's method with suitable initial values (see Appendix).

Figure 5 compares computed eigenvalues μ_1 and μ_2 of the monodromy matrix $\hat{X}(T)$ of unstable periodic solutions

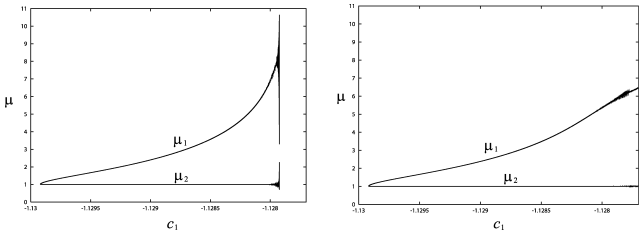

(a.1) the simple shooting method (a.2) the proposed method

(a) $\rho = 1$

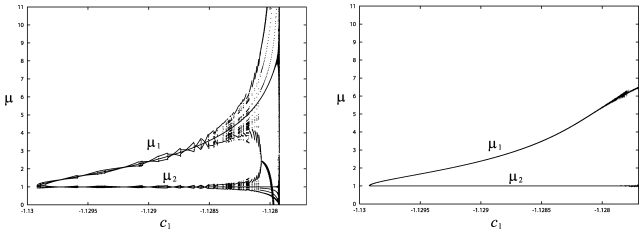

(b.1) the simple shooting method (b.2) the proposed method

(b) $\rho = 100$

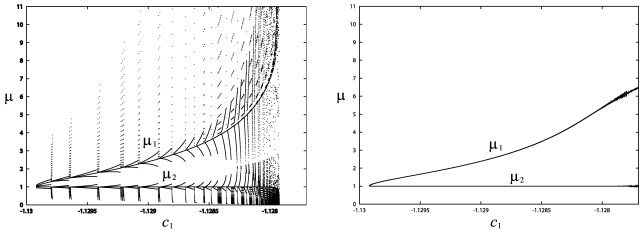

(c.1) the simple shooting method (c.2) the proposed method

(c) $\rho = 10000$

Fig. 5 Computed eigenvalues μ_1 and μ_2 of the monodromy matrix $\hat{X}(T)$ for $x_0 \in \Sigma_+$ and ρ =1, 100 and 10000. (a.1), (b.1) and (c.1) show the real parts of $\mu_{1,2} \in \mathbb{C}$ by the simple shooting method which had non-zero imaginary parts. (a.2), (b.2) and (c.2): $\mu_{1,2} \in \mathbb{R}$ by the proposed method which had no imaginary parts.

of Eq. (17) using the simple shooting method and the proposed method with $\hat{x}_0 \in \Sigma_+$ and $\rho = 1$, 100 and 10000. These periodic solutions correspond to those in Fig. 4. It should be noted that, for $\hat{x}_0 \in \Sigma_-$, both methods gave the same results as those in Fig. 4(a), and that Fig. 5 shows only the results for $\hat{x}_0 \in \Sigma_+$. The imaginary parts of the computed eigenvalues by the simple shooting method were not zero for $\hat{x}_0 \in \Sigma_+$ and $\rho = 100$ and 10000, and those by the proposed method were zero. Since the exact eigenvalues are real as shown in Eq. (14), Fig. 5 shows the real parts of the computed eigenvalues. These results show that the computed eigenvalues by the simple shooting method depend on ρ sensitively, although the exact eigenvalues are independent of ρ as shown in Eq. (18). This results from increase of errors in the computed monodromy matrix $\tilde{X}(\tilde{T})$ due to the coordinate transformation (16). That is, for $\tilde{X}(\tilde{T})$ for $\rho = 1$ in the form

$$\tilde{X}(T) \simeq \begin{pmatrix} \lambda & \delta \\ \nu & 1 \end{pmatrix} \quad (|\delta| \ll 1), \tag{21}$$

the corresponding $\hat{\tilde{X}}(\tilde{T})$ for $\rho > 1$ is given by

$$\hat{\tilde{X}}(\tilde{T}) = Q^{-1}\, \tilde{X}(\tilde{T})\, Q \simeq \begin{pmatrix} \lambda & \rho\delta \\ \frac{1}{\rho}\nu & 1 \end{pmatrix}. \tag{22}$$

For a large value of ρ, the absolute value of the (2,1) element ($\simeq \nu/\rho$) of $\hat{\tilde{X}}(\tilde{T})$ can be reduced, but the (1,2) element ($\simeq \rho\delta$) can be away from zero. This causes sensitive dependence of computed eigenvalues by the simple shooting method on ρ. On the other hand, in the proposed method, Newton's method is applied for Eq. (20), $H(u, \tau) = 0$, such that the periodic boundary condition (9) is satisfied with certain accuracy. This means that the iteration in Newton's method is repeated until the second column of $\hat{\tilde{X}}(\tilde{T})$ is close to the exact one $(0, 1)^\top$. That is the reason why the computed eigenvalues by the proposed method do not depend on ρ and also satisfy Theorem 2(a), namely $\mu_2 = 1$.

These results suggest that the proposed method using the periodic boundary condition (9) produces more accurate eigenvalues of the monodromy matrix than the simple shooting method using (6) and do not depend on the coordinate transformation. But accurate approximate solutions $\tilde{x}_0$ and $\tilde{T}$ for Eq. (9.a) are not necessarily those for Eq. (6.a), although the exact solutions x_0^* and T^* for Eq. (6.a) satisfy Eq. (9.a). Next section discusses this in more detail.

5. Discussions

5.1 Effects of Accuracy of Solutions on Periodic Boundary Conditions

This section considers effects of errors of approximate solutions $\tilde{x}_0$ and $\tilde{T}$ on two periodic boundary conditions (6.a) and (9.a), namely

$$P_1(T, x_0) = \varphi(T, x_0) - x_0 = 0, \tag{23}$$

and

$$P_2(T, x_0) = X(T)f(x_0) - f(x_0) = 0. \tag{24}$$

When the exact solutions x_0^* and T^* are expressed as $x_0^* = \tilde{x}_0 + \Delta x_0$ and $T^* = \tilde{T} + \Delta T$, respectively, these periodic boundary conditions can be expanded as follows:

$$\begin{aligned} &P_1(\tilde{T} + \Delta T, \tilde{x}_0 + \Delta x_0) \\ &\quad = \varphi(\tilde{T}, \tilde{x}_0) - \tilde{x}_0 + \alpha_1 \Delta T + A_1 \Delta x_0 \\ &\qquad + \mathrm{O}(\Delta T^2, {\Delta x_0}^2) \\ &P_2(\tilde{T} + \Delta T, \tilde{x}_0 + \Delta x_0) \\ &\quad = X(\tilde{T})\, f(\tilde{x}_0) - f(\tilde{x}_0) + \alpha_2 \Delta T + A_2 \Delta x_0 \\ &\qquad + \mathrm{O}(\Delta T^2, {\Delta x_0}^2) \end{aligned} \tag{25}$$

where

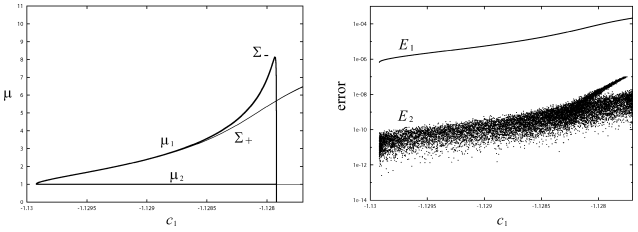

(a) eigenvalues μ_1 and μ_2 (b) errors E_1 and E_2 ($x_0 \in \Sigma_+$)

Fig. 6 Computed eigenvalues μ_1 and μ_2 of the monodromy matrix $X(T)$ using the proposed method and errors E_1 and E_2 of periodic boundary conditions. In (a), thin line : $x_0 \in \Sigma_+$ and thick line : $x_0 \in \Sigma_-$. $\rho = 100$.

$$\begin{aligned}
\alpha_1 &= f(\varphi(\tilde{T}, \tilde{x}_0)),\\
\alpha_2 &= \frac{\partial f}{\partial x}(\varphi(\tilde{T}, \tilde{x}_0))\, X(\tilde{T})\, f(\tilde{x}_0),\\
A_1 &= X(\tilde{T}) - I,\\
A_2 &= \frac{\partial^2 \varphi}{\partial {x_0}^2}(\tilde{T}, \tilde{x}_0)\, f(\tilde{x}_0) + X(\tilde{T})\, \frac{\partial f}{\partial x}(\tilde{x}_0) - I.
\end{aligned} \tag{26}$$

If norms of coefficients α_j or A_j ($j = 1, 2$) are large, then errors of periodic conditions $\|P_j(T^*, x_0^*) - P_j(\tilde{T}, \tilde{x}_0)\|$ can be large even with small ΔT or Δx_0. Hence, in some cases, more accurate numerical integrators such as implicit Runge-Kutta methods do not help us significantly reduce the errors of periodic conditions (23) and (24).

When errors of computed eigenvalues are large as shown in Fig. 4(b), the norms of these coefficients α_j or A_j ($j = 1, 2$) can be large. For example, the maximum norms $\|\alpha_{1,2}\|$ of the coefficients of ΔT for $x_0 \in \Sigma_-$ at $c_1 \simeq -1.1279$ in Fig. 4 were $\|\alpha_1\| = \mathrm{O}(1)$ and $\|\alpha_2\| = \mathrm{O}(1)$. On the other hand, these for $x_0 \in \Sigma_+$ were $\|\alpha_1\| = \mathrm{O}(1)$ and $\|\alpha_2\| = \mathrm{O}(10^8)$. These results indicate that the periodic boundary condition $P_2(T, x_0) = 0$ is more sensitive to the errors ΔT and Δx_0 than $P_1(T, x_0) = 0$. Also, a critical property of the monodromy matrix, Theorem 2(a), is directly related to the periodic boundary condition $P_2(T, x_0) = 0$. These make the proposed method reliable.

The aim of this work is to develop a numerical method for Eqs. (1) and (2), which preserves some critical properties of the monodromy matrix $X(T)$, in other words some geometrical features of these equations. In this sense, some ideas of geometric numerical integration [4], in particular numerical integrators on manifolds, are related to this work. It is because suitable choice of local coordinates may reduce the magnitude of the coefficients α_2 and A_2 given by differentiation with respect to x and x_0. This will be considered in future works.

5.2 Errors of the Periodic Boundary Conditions

Figure 6(a) compares computed eigenvalues μ_1 and μ_2 using the proposed method for $x_0 \in \Sigma_+$ with those for $x_0 \in \Sigma_-$. These results show that one of the computed eigenvalues, μ_1, for $x_0 \in \Sigma_+$ disagrees with that for $x_0 \in \Sigma_-$ at $c_1 \simeq -1.128$ where the corresponding periodic solution is near a homoclinic orbit. Thus Theorem 2(b) is not satisfied. This disagreement indicates that it is not straightforward to make approximate solutions $\tilde{x}_0$ and $\tilde{T}$ meet both periodic boundary conditions, (6.a) and (9.a), with certain accuracy in numerical computation, as stated in the end of Sect. 4.3. In order to consider this, define the error of the periodic boundary condition (6.a) by

$$E_1 = \|\varphi(T, x_0) - x_0\|, \tag{27}$$

and that of (9.a) by

$$E_2 = \|X(T) f(x_0) - f(x_0)\|, \tag{28}$$

respectively. Here $\|\ \|$ denotes the maximum norm. Figure 6(b) shows these two errors E_1 and E_2 for $x_0 \in \Sigma_+$ in Fig. 6(a). It is found that $E_2 < 10^{-7}$ which agrees with the convergence condition of Newton's method for Eqs. (20), $H(u, \tau) = 0$, and that $E_1 > 10^{-5}$ at $c_1 \simeq -1.128$ because E_1 is not directly controlled in this computation. On the other hand, for $x_0 \in \Sigma_-$ in Fig. 6(a), both errors E_1 and E_2 were less than 10^{-7}. These show that the error E_1 causes disagreement of the eigenvalue μ_1 in Fig. 6(a), and that the computed results for $x_0 \in \Sigma_-$ are more accurate than those for $x_0 \in \Sigma_+$. It should be noted that the computed eigenvalues for $x_0 \in \Sigma_-$ in Fig. 6(a) agree with those by the simple shooting method in Fig. 4(a).

Although only Σ_+ and Σ_- on the x-axis are used in this work, choice of the position of the cross-section Σ is arbitrary on the orbit. Also we can utilize the multiple shooting method, instead of the simple shooting method, with (9.a) and some highly accurate numerical scheme for ordinary differential equations. This work did not consider these, in order to focus on the periodic conditions. These will be examined in future works.

6. Conclusions

This work has considered boundary conditions used in numerical methods for stability analyses of periodic solutions of ordinary differential Eq. (1). Stability of a periodic solution is determined by the monodromy matrix which is a solution of the corresponding variational Eq. (2). This work proposes a numerical method using a periodic boundary condition (9.a) for vector fields, which takes one of critical properties of the monodromy matrix, Theorem 2(a), into consideration. Numerical examples for the Van der Pol - Duffing Eq. (10) demonstrate that the proposed method produces more accurate eigenvalues of the monodromy matrix than the simple shooting method using the commonly used periodic boundary condition (6.a).

It is also shown in numerical examples that, for periodic solutions near a homoclinic orbit, the proposed method fails to catch another critical property of the monodromy matrix, Theorem 2(b). This remains as a future work.

References

[1] G. Dangelmayr and J. Guckenheimer, "On a four parameter family of

planar vector fields," Arch. Ration. Mech. Anal., vol.97, pp.321–352, 1987.
[2] T.F. Fairgrieve and A.D. Jepson, "O.K. Floquet multipliers," SIAM J. Numer. Anal., vol.28, no.5, pp.1446–1462, 1991.
[3] J. Guckenheimer and B. Meloon, "Computing periodic orbits and their bifurcations with automatic differentiation," SIAM J. Sci. Comput., vol.22, no.3, pp.951–985, 2000.
[4] E. Hairer, C. Lubich, and G. Wanner, Geometric Numerical Integration: Stucture-Preserving Algorithms for Ordinary Differential Equations, 2nd ed., Springer, 2006.
[5] Y.A. Kuznetsov, Elements of Applied Bifurcation Theory, 2nd ed., Springer, 1998.
[6] K. Lust, "Improved numerical Floquet multipliers," Int. J. Bifurcation and Chaos, vol.9, no.11, pp.2389–2410, 2001.
[7] C. Robinson, Dynamical Systems, 2nd ed., CRC Press, 1999.
[8] R. Seydel, "New methods for calculating the stability of periodic solutions," Comput. Math. Applic., vol.14, no.7, pp.505–510, 1987.

Appendix: Computation of the Jacobian Matrix in Newton's Method

In Newton's method for Eq. (13), $F(u,\tau)=0$, the unknown variables u and τ are modified by $u+\Delta u$ and $\tau+\Delta\tau$ using

$$\begin{pmatrix} \dfrac{\partial F_1}{\partial u} & \dfrac{\partial F_1}{\partial \tau} \\ \dfrac{\partial F_2}{\partial u} & \dfrac{\partial F_2}{\partial \tau} \end{pmatrix} \begin{pmatrix} \Delta u \\ \Delta \tau \end{pmatrix} = - \begin{pmatrix} F_1(u,\tau) \\ F_2(u,\tau) \end{pmatrix}, \tag{A·1}$$

where the Jacobian matrix is given by

$$\begin{pmatrix} \dfrac{\partial F_1}{\partial u} & \dfrac{\partial F_1}{\partial \tau} \\ \dfrac{\partial F_2}{\partial u} & \dfrac{\partial F_2}{\partial \tau} \end{pmatrix} = \left. \begin{pmatrix} \dfrac{\partial \varphi_1}{\partial x_0^1} - 1 & \dfrac{\partial \varphi_1}{\partial t} \\ \dfrac{\partial \varphi_2}{\partial x_0^1} & \dfrac{\partial \varphi_2}{\partial t} \end{pmatrix} \right|_{t=\tau, x_0=(u,0)}, \tag{A·2}$$

with $x_0=(x_0^1,x_0^2)$. Here $(\partial\varphi_j/\partial x_0^1)\big|_{t=\tau,x_0=(u,0)}$ for $j=1,2$ can be obtained using Eq. (2) and the Runge-Kutta method, and $(\partial\varphi_j/\partial t)\big|_{t=\tau,x_0=(u,0)} = f_j(\varphi(\tau,(u,0)))$ for $j=1,2$.

Similarly, Δu and $\Delta\tau$ for Eq. (20), $H(u,\tau)=0$, are given by

$$\begin{pmatrix} \dfrac{\partial H_1}{\partial u} & \dfrac{\partial H_1}{\partial \tau} \\ \dfrac{\partial H_2}{\partial u} & \dfrac{\partial H_2}{\partial \tau} \end{pmatrix} \begin{pmatrix} \Delta u \\ \Delta \tau \end{pmatrix} = - \begin{pmatrix} H_1(u,\tau) \\ H_2(u,\tau) \end{pmatrix} \tag{A·3}$$

where

$$\begin{aligned} \frac{\partial H_1}{\partial u} &= \sum_{j=1}^{2} \frac{\partial \varphi_2}{\partial x_0^j} \frac{\partial f_j}{\partial x^1}(x_0) + \sum_{j=1}^{2} \frac{\partial^2 \varphi_2}{\partial x_0^1 \partial x_0^j} f_j(x_0) \\ &\quad - \frac{\partial f_2}{\partial x^1}(x_0), \\ \frac{\partial H_2}{\partial u} &= \sum_{j=1}^{2} \frac{\partial \varphi_1}{\partial x_0^j} \frac{\partial f_j}{\partial x^1}(x_0) + \sum_{j=1}^{2} \frac{\partial^2 \varphi_1}{\partial x_0^1 \partial x_0^j} f_j(x_0), \\ \frac{\partial H_1}{\partial \tau} &= \sum_{j,k=1}^{2} \frac{\partial f_2}{\partial x^j}(\varphi_\tau(x_0)) \frac{\partial \varphi_j}{\partial x_0^k} f_k(x_0), \end{aligned}$$

$$\frac{\partial H_2}{\partial \tau} = \sum_{j,k=1}^{2} \frac{\partial f_1}{\partial x^j}(\varphi_\tau(x_0)) \frac{\partial \varphi_j}{\partial x_0^k} f_k(x_0), \tag{A·4}$$

at $t=\tau$ and $x_0=(u,0)$. Here $x=(x^1,x^2)$ and $\partial^2\varphi_i/\partial x_0^p \partial x_0^q$ for $i,p,q=1,2$ can be obtained using

$$\begin{aligned} &\frac{\mathrm{d}}{\mathrm{d}t}\left(\frac{\partial^2 \varphi_i}{\partial x_0^p \partial x_0^q}\right) \\ &= \sum_{j=1}^{2} \frac{\partial f_i}{\partial x^j} \frac{\partial^2 \varphi_j}{\partial x_0^p \partial x_0^q} + \sum_{j,k=1}^{2} \frac{\partial^2 f_i}{\partial x^j \partial x^k} \frac{\partial \varphi_j}{\partial x_0^p} \frac{\partial \varphi_k}{\partial x_0^q}, \end{aligned} \tag{A·5}$$

with $\left.\dfrac{\partial^2 \varphi_i}{\partial x_0^p \partial x_0^q}\right|_{t=0} = 0.$

Sunao Murashige received the B.E., M.E., and Dr. Eng. degrees from the University of Tokyo, Japan, in 1986, 1988, and 1991, respectively. His research interests are numerical calculation and dynamical system.